Vision based road profile estimation for preview-controlled vehicle suspension systems

Mert Büyükköprü * ID
Groupe Renault, Balat OSB. Mavi Cd 5. Sk. No:1, Bursa, Türkiye, mert.buyukkopru@renault.com

Erdem Uzunsoy ID
Bursa Technical University, Mechanical Engineering Department, 16310, Bursa, Türkiye, erdem.uzunsoy@btu.edu.tr

Xavier Mouton ID
Groupe Renault, 122 Av. du Général Leclerc, 92100 Boulogne-Billancourt, France, xavier.mouton@renault.com

* Corresponding Author

Abstract:

In this paper, a vision-based road profile estimation method was studied for the control of semi-active and active suspension systems. For the purpose, a monocular camera was used to collect data from the road tests to develop a logic to convert the camera measurements into the road profile data. For the generation of the road profile, alignment of the different sets of camera measurements and their coherence were expressed. Importance of the sensor and process noise removal were shown in recognition of the high frequency content of the road profile, which was a particular interest of the study. Additionally, a density-based clustering algorithm was taken into account to cluster the measured points vertically, to remove the process and sensor noise. The density-based clustering method reduced the noises and allowed detection of the high and low frequency contents of the road.

Keywords: Clustering, Estimation, Road profile recognition

1. INTRODUCTION

Ride dynamics of road vehicles has been developed based on the industry requirements and human vibration sensitivity thresholds. Road surface characteristics have significant effects on vehicle ride and handling dynamics[1]. Estimation of the road surface characteristics may help to improve the comfort and hazard avoidance system of the vehicles [2]. There has been plenty of studies to estimate road profiles since the idea of electronic suspension control was developed. Most of these studies have been relied on vibration-based approaches such as evaluation of the root mean square of the acceleration measurements on the vehicle body and wheels [3–5] . Vibration based approaches inherently give results as soon as the tyres passed over a vibratory input such as bumps and potholes on their trajectory. In these methods, starting from a moment that a notable input can be detectable visually, there is an important time gap without any automatic control action. In fact, this gap can be transformed into a highly valuable period with some accumulated data depending on the preview information of the road profile characteristics, therefore, further improvements can be done on the level of comfort. At this point, preview control logic has been introduced as an acceptable improvement to the system. However, when the idea of the preview control logic was first developed by Bender [6] almost five decades ago, the contactless measuring technology was not at the desired level [7].

Recently developed sensing devices, such as Lidar, Stereo and Monocular Cameras, have made the estimation of road profiles before passing the vehicle over its trajectory, possible [8]. However, research studies on preview control have mostly been focused on the basic principles and the improvements of predictive control logic and preview control itself rather than the source of disturbance [9–11], whereas, the road profile recognition procedure is the main element in realising the preview control approach, in practice.

One of the first studies related to the road profile implementation for the purpose of preview control of the vehicle body was done by Streiter [12]. Schindler used a lidar sensor to gather the preview information, due to the accuracy compared to an ultrasonic sensor or an ADAS camera. In that study, a regression analysis method was proposed to construct the road profile from a point cloud and the least square approximation method was used to match the consecutive sensor measurements regarding to ego motions of the vehicle [13]. In another study, a compact ADAS lidar was preferred for an active suspension system, and ego motions were compensated by the chassis control systems' sensor measurements [14] . Gong et al. utilized a lidar sensor to recognize an off-road profile. In the study, measurement variations between consecutive steps were compensated using a gyro near the lidar. Then, dense lidar data were denoised and interpolated to generate the road profile and determine the road class [15]. Similar to the works done using lidar sensors, the best fitting of the consecutive images of a camera also allows the estimation of the ego-motion. Stein et al. focused on estimating the ego-motion by using a camera. The previous and current images were compared and applied the best fit within the initial guess of the motion considering the longitudinal displacement, measured by a speedometer [16].

Göhrle et al. used a stereo camera to recognise the low frequency-long wavelength road profiles. In the study, two consecutive measurements were used to align actual and previous measurements, as in Schindler's approach. The authors also used statistical approaches such as the maximum-likelihood and probability density functions to estimate the possible mean value of the several measurements of a point in one measurement window [17]. In another study, a multi-purpose stereo camera was utilised to control the actuator in the frequency range from 0.5 to 5Hz.

Scanning results of the camera was accumulated during each 60.3ms period, and the camera could scan the road up to 15m in front of the vehicle. Multiple measurements were combined by a statistical method

aiming to improve the accuracy of the road profile estimation. However, the details of the method have not been disclosed, publicly [18].

A camera's road surface evaluation success depends on the road surface texture, lighting reflectance, weather conditions, and ego motion [19]. Therefore, confidence values are assigned to height values those measured with camera by various methods [20]. There are many ways in the literature to calculate the confidence of the camera's measurements, such as left-right difference and Naive peak ratio [21]. Thus, when the measurement scores are low, statistical methods can be used to lessen the impact of some of the low score measurements to have a more reliable road profile.

If a road profile recognition procedure by cameras is considered in two steps, the first step is image processing and the elevation profile creation and the second step is the conversion of the obtained elevation data to the road profile. In the literature, studies have generally been conducted to obtain height data through image processing[22–24]. The information available on how to combine elevation data to create a road profile, effectively, is highly limited. For instance, only the application of windowing approach can be seen in the references [17,25]. The method divides a cloud of sensor measured road surface points into equal segments on the longitudinal x-axis.

The same or very close points on the path are measured more than once. The points, those have been measured multiple times and being close together, naturally form densities in certain regions, namely, "natural clusters" and the densities may not be identical in shape. As will be discussed in more detail in the following sections, this is where the windowing approach has its main weakness in providing the highest possible accuracy. Clustering methods can be used to associate measurement points with each other. In this context, density-based spatial clustering of applications with noise algorithm , DBSCAN, was preferred to establish a relationship between the points by making use of the natural clusters formed by these points those are close to each other [26]. It is probably the most considerable density-based method as of today [27], however, DBSCAN has not been used for the purpose of road profile recognition studies. On the other hand, it is the control strategy chosen against the body motions and actuator bandwidth determines the type of surface scanning strategies [28]. For instance, a typical skyhook control strategy can attenuate the vibrations of the body with frequencies up to 3 Hz. From the handling point of view, whereas, the wheel resonance frequency is generally between about 8 and 10 Hz [29]. Usually, for a low bandwidth fully active suspension, the primary aim is to keep the vehicle body as stable as possible so that the higher road frequencies, which are out of the actuator control bandwidth, are eliminated. On the contrary, getting the information of the higher road frequencies can be an advantage for disturbance rejection for the semi-active suspension type actuators. On the other hand, it is difficult to recognise the high-frequency content of the road profile as the data processing for the road profile generation causes additional process noises by the current road profile generation methods.

This paper aims to use high frequency content besides the low frequency content of the road profile. Therefore, unlike the windowing approach used in the literature, a density based spatial clustering of applications with noise (DBSCAN) algorithm was adapted to avoid creating process noise while converting consecutive measurements to the road profile [31]. This study is among the first to investigate the optimisation of road profile detection results by spatially clustering detection results of different road tests, in the literature. For the purpose, a monocular camera was used to collect data from the road tests to develop a logic to convert the camera measurements into road profile data. The camera itself carries out the image processing for the spatial referencing of the consecutive measurements with respect to the previous measurements thanks to the estimation of the ego-motion in particular. In addition, image processing is a black box as it is the supplier's know-how. Therefore, we were interested in the road profile generation step with the image processed data rather than image processing. For the

generation of the road profile, the alignment of the different sets of camera measurements were expressed and sensor and process noise prevention, in particular, were shown.

2. GENERATION OF THE ROAD HEIGHT PROFILE

2.1. Measurement of Road Height Profile

A sensor mounted on the windshield measured the road surface from 5m to 16m in front of the front axle for both left and right wheels at each time step, as in figure 1. The sensor consecutively generated the measurement points while the vehicle was moving. The generated points were non-uniform, and they must be arranged to increase the measurement accuracy.
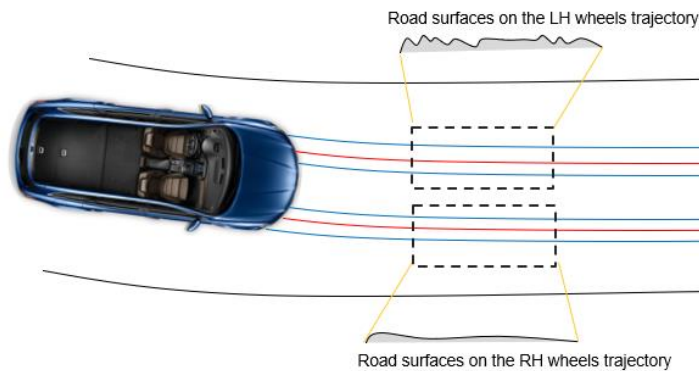

Figure 1. Measurement zone on the trajectory of the vehicle.

2.2. Alignment of the Points

At each time step, a new set of measurement was created. Measurement sets developed a points cloud, which includes distance and height data of the points $(X_i^j, Z_i^j \ldots X_{i+k}^{j+n}, Z_{i+k}^{j+n})$, depending on the vehicle speed as in Figure 2. A positioning algorithm located the next point cloud corresponding to its distance just after the previous measurement. As the vehicle was moving forward, the same points on the road surface (or the closest points on the same surface) were measured several times. Therefore, the same or closer measurement points were overlapped, in a scattered manner. At each step, the distance between the measurement points $(X_{i+1}^{j+1} - X_i^j)$ was different due to the changing vehicle speed during the image processing. First, measured points in the cloud were sorted from the closest to the farthest according to the vehicle's front axle center.
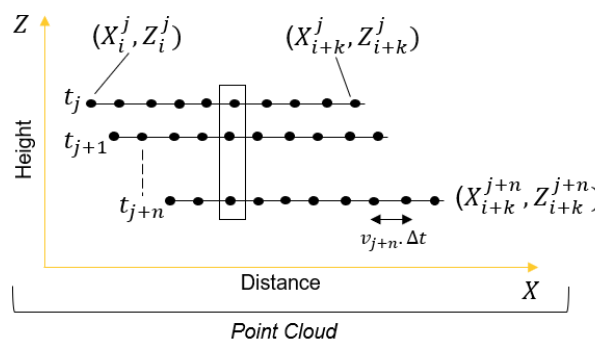

Figure 2. Measurement point relation in the point cloud.

Then, the measurement points were split into the segments to determine the points to be averaged to find the most probable height from different measurements. For example, a for loop can group the points into the cells for a fixed window length. As it can be seen in figure 3, the fixed-length windows split the overlapped points into the segments. The window length defines the resolution of the final profile. If the length is too short, the number of iterations increases the size of the matrix, which includes the distance, height, and confidence values. Otherwise, a too-long window length may reduce the resolution while reducing the number of iterations.
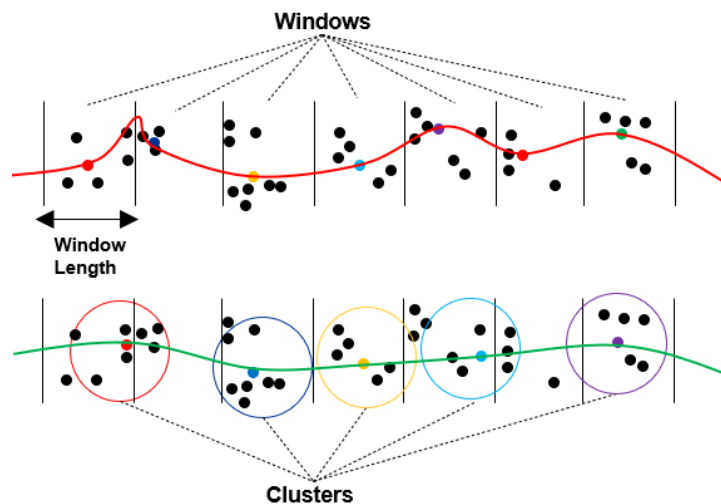

Figure 3. Windowing approach and DBSC comparison.

2.3. Density Based Clustering of Points Cloud

Using the fixed window length and averaging approach alone was not enough to regulate the scattered points in the clouds. Even though the intervals between the measured points were equal in x-direction in a measurement set, each measurement set had different intervals due to the variations in vehicle speed. Therefore, the measurement points were not aligned on the vertical and horizontal plane. When the point cloud was split into segments by windows, as the windowing approach does not consider the proximity between the points, some windows include more points than others. These deviations in the x-direction caused additional complexity, which was a redundant junction in the signal. If the distance between the closer points in the horizontal direction is lower than the theoretically allowable minimum distance due to the camera capability, then, the road signal might include an additional noise. However, the shape of the road profile and window length are also important factors; if the window length is too small, then, unwanted artificial noises occur.

In terms of profile evaluation considering relatively high frequencies, the redundant junctions in the profile produce artificial high-frequency content due to data processing. Therefore, the points, which were to be averaged together could be identified globally in the interconnected point clouds. In regard to this matter, DBSCAN is a powerful algorithm that allows clustering points due to their distribution in a plane by also defining points as the core, neighbour, and noise [31]. As a result, to identify the groups of points "to be averaged", a Density-based spatial clustering of applications with noise (DBSCAN) was proposed.

In this technique, neighbour points were located around the core points, and a minimum number of points (minpts) in the cluster was defined as density threshold, and the radius (ε) was the neighbourhood range. The minpts was defined according to the number of the measurements. Radius (ε) was defined according to the desired resolution, which can be a variable value according to vehicle speed. DBSCAN checks each point in a loop. In order to define the core point, at least minimum points, minpts, must be

within the distance of radius (ε). If it satisfies this condition, it is, then, the core point. If it does not, it is either a noise or a border point. If the point inside the circle is around the core point, it is a border point. Otherwise, it is a noise. Finally, all clusters were labelled, and noise and neighbour points were assigned according to DBSCAN algorithm steps. Basic pseudo code of original DBSCAN is given in table 1 [32]. When the clusters were obtained, the averaging could be applied to all cluster members according to the confidence values.

Table 1 pseudocode of original sequential DBSAN algorithm

```
Input: DB: Database
Input: ε: Radius Input: minPts: Density threshold
Input: dist: Distance function
Data: label: Point labels, initially undefined
 1  foreach point p in database DB do // Iterate over every point
 2  if label(p) undefined then continue // Skip processed points
 3  Neighbours N ← RangeQuery(DB, dist,p,ε) // Find initial neighbours
 4  if |N | < minPts then // non-core points are noise
 5      label(p) ← Noise
 6      continue
 7  c ← next cluster label // Start a new cluster
 8  label(p) ← c
 9  Seed set S ← N \ {p} // Expand neighbourhood
10  foreach q in S do
11      if label(q) = Noise then label(q) ← c
12      if label(q) undefined then continue
13      Neighbours N ← RangeQuery(DB, dist,q,ε)
14      label(q) ← c
15      if |N | < minPts then continue // Core-point check
16      S ← S ∪ N
```

2.4. Sensor Noise Reduction

Any particular point having different height values could affect the final profile approximations. The height deviations could be reduced using averaging techniques. Any particular point's confidence values can be used in averaging as weighting factors; thus, more reliable measurements contribute more than less reliable measurements. A simple weighted arithmetic mean method (Equation 1) was applied for the purpose, and weighting factors were selected concerning the confidence value of the points. Weight factors are $\omega_i = \{\omega_1, \omega_2, \ldots, \omega_n\}$ and for non-empty $\omega_i > 0$ and $Z_i = \{Z_1, Z_2, \ldots, Z_n\}$ are measured heights of each of the points. The measurement points were clustered around the core points. Then, the height of the points in the clusters were averaged in vertical axis according to their individual confidences, as in figure 4.

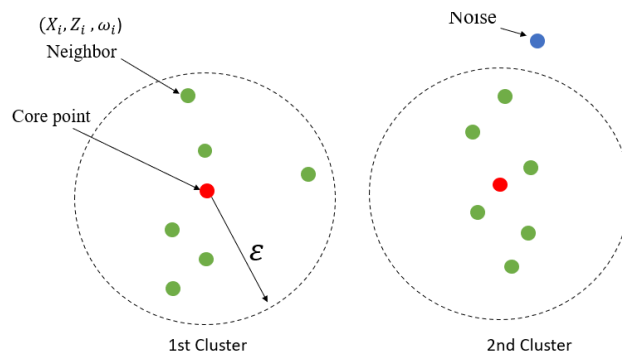$$\bar{Z} = \frac{\sum_{i=1}^{n} \omega_i \cdot Z_i}{\sum_{i=1}^{n} \omega_i} \qquad (1)$$

Figure 4. Different length measurements in X and Z directions with DBSC clustering.

2.5. Distance to Time Domain Transformation

Since the processed data is in the distance domain, it must be converted to the time domain for filtering and to calculate the time to reach the target road surface. X_k is the distance of the measured point from the center of the front axle. The conversion from distance domain was applied using $X_k = f(t_k, V_k) \cup f(z_k)$, which is a function of time, speed, and height profile. Any X values can be converted by the integration of vehicle speed in Equation 2. Calculated X_k could be matched with its corresponding height value as $(X_k, Z_k) \equiv (t_k, Z_k)\, Z_k$, using the linear interpolation given in Equation 3.

$$t_k = \sum_{k}^{p}(X_k/V_k) \tag{2}$$

$$Z_k = Z_a + (Z_b - Z_a) \times \frac{(X_k - X_a)}{(X_b - X_a)}\ at\ point\ (X_k) \tag{3}$$

3. ROAD DATA ACQUSITION AND RESULTS

To realize the main purpose of this study, road tests were performed on different road profiles shown in figures 5, 6. The measurement confidence scores were given at the bottom of figures 5 and 6. The prototype camera assembled on the windshield of the test car with 100° field of view and 1820 x 940 pixels, can be seen in figure 5. The vehicle speed was 44 kph and 15kph at the first and second track which are shown in figures 6 and 7, respectively.

A data logger was used to record the prototype camera outputs, and data was sampled at 300Hz. Next, the recorded data were processed offline for comparison. The road profile shown in figure 6 was stone paved, and measurement confidence scores were substantially greater than 3 on a scale of 0 to 5, indicating increasing reliability from small to large.

Figure 5. The test vehicle with monocular camera in red circle.

In figure 7, the effect of the speed bump shape can be seen clearly, and the measurement confidence decreased to zero around 14m. Both camera outputs were processed to compare DBSCAN and windowing approaches. Eps, ε, value and window length were set to 0.015m and 0.005m, respectively. minpts value was set to 2 for DBSCAN. The results of both the windowing and DBSCAN approaches for the first test track can be seen in figure 8. Unlike the windowing approach, which included artificial noises, DBSCAN produced a smooth profile.
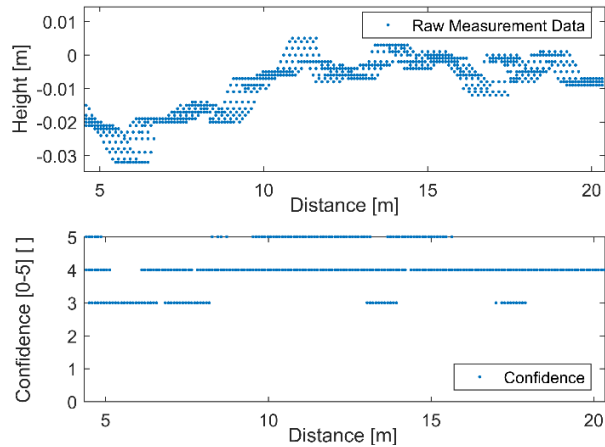

Figure 6. Raw Measurement data for the first test track.

In figure 9, on the other hand, some process noise can be seen, clearly, as a result of the windowing approach. It can be seen that the distance between the points increases depending on the sudden changes on the shape of measured surface. The fixed-length windowing approach causes a sudden change in the profile at 14m. Low amplitude noise from the process could be seen across almost the entire profile in the detailed view of figure 8.
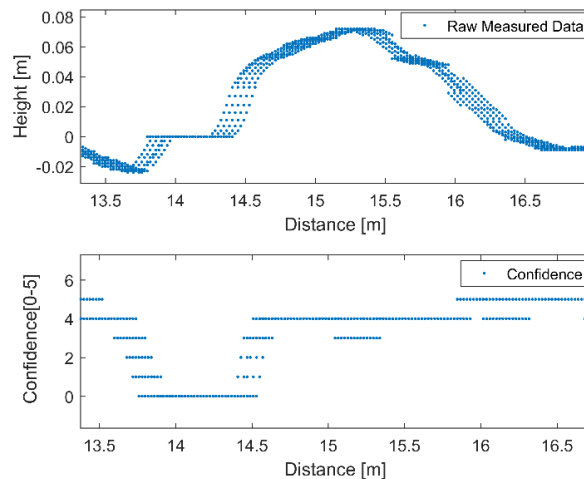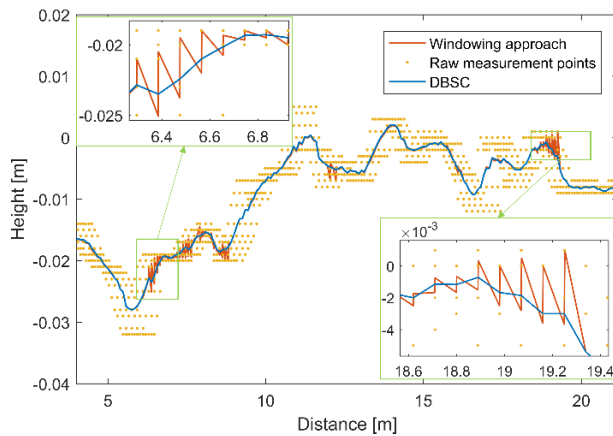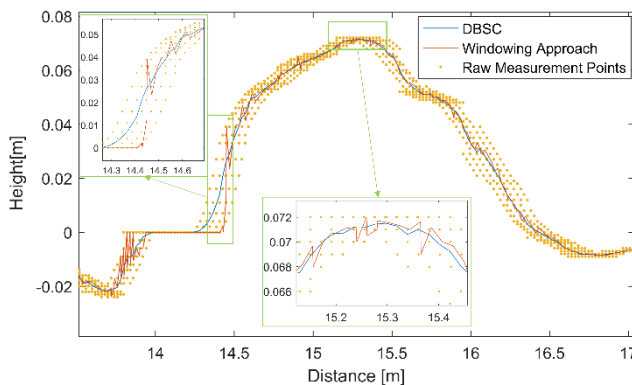

Figure 7. Measurement data for the second test track.

ε =0.015
minpts=2
window length=0.005m on the LH wheel trajectory

Figure 8. DBSC and windowing approach comparison

ε =0.015
minpts=2
window length=0.005m for a speed bump on the LH wheel trajectory

Figure 9. DBSC and windowing approach comparison

4. CONCLUSION

In this study, the DBSCAN algorithm was adapted to generate road profiles from the multiple set of scattered points clouds, which were provided by a monocular camera. The principal idea was to compare the windowing approach and DBSCAN for the road profile evaluation in terms of detectability of the road profile's low and high frequency content within the provided sensor limits.

The main problem was aligning the points against their variation to find the most probable height due to the confidence of the camera measurements. The camera's accuracy caused deviations in the height measurement. Using the DBSCAN method reduced the processing noises. Thus, it allowed the detection of high-frequency road profile contents without any additional filtering, as a result of the absence of additional process noise.

Window length of 0.005m was chosen based on the *trial-and-error* method to obtain accurate and less noisy results. A larger value will obviously reduce the road profile detection accuracy. However, this value can be determined according to the average of the distances of the points to each other in the point set. The minpts value can be chosen to be at least two. Another factor in the use of DBSCAN was the determination of the radius (ε). If the radius is not small enough, the accuracy of the profile will decrease. However, if it is too small, the number of clusters will be increased, which may increase the computational cost, and it may assign some of the points those are not homogeneously distributed as noise, thus, resulting in data loss. In order to avoid the problems such as loss of accuracy and data, the radius can

be determined according to the average of the distances of the points in the x and y axis directions. Since the distance between the points is calculated depending on the instantaneous vehicle speed, radius (ε) can be formulated as a function of vehicle speed. Therefore, more robust road profile development can be achieved.

Acknowledgement

7. REFERENCES

[1] Wong JY. Theory of Ground Vehicles. 3rd ed. Ottawa, Canada: Wiley; 2001.

[2] Guerrero-Ibáñez J, Zeadally S, Contreras-Castillo J. Sensor Technologies for Intelligent Transportation Systems. Sensors, 2018;18:1212. DOI:10.3390/s18041212.

[3] Ward CC, Iagnemma K. Speed-independent vibration-based terrain classification for passenger vehicles. 2009;47:1095–1113. DOI: 10.1080/00423110802450193.

[4] Qin Y, Dong M, Zhao F, et al. Road profile classification for vehicle semi-active suspension system based on Adaptive Neuro-Fuzzy Inference System. Proc IEEE Conf Decis Control. 2015;54rd IEEE:1533–1538. DOI:10.1109/CDC.2015.7402428.

[5] Qin Y, Langari R, Wang Z, et al. Road profile estimation for semi-active suspension using an adaptive Kalman filter and an adaptive super-twisting observer. Proc Am Control Conf. 2017;973–978. DOI:10.23919/ACC.2017.7963079.

[6] Bender EK. Optimum Linear Preview Control With Application to Vehicle Suspension. J Basic Eng. 1968;90:213–221. DOI:10.1115/1.3605082.

[7] Hac A. Optimal Linear Preview Control of Active Vehicle Suspension. Vehicle System Dynamics. 1992;21:167–195. DOI:10.1080/00423119208969008.

[8] Oniga F, Nedevschi S, Meinecke MM, et al. Road surface and obstacle detection based on elevation maps from dense stereo. IEEE Conf Intell Transp Syst Proceedings, ITSC. 2007;859–865. DOI:10.1109/ITSC.2007.4357734.

[9] Mehra RK, Amin JN, Hedrick KJ, et al. Active suspension using preview information and model predictive control. IEEE Conf Control Appl - Proc. 1997;860–865. DOI:10.1109/CCA.1997.627769.

[10] Ryu S, Kim Y, Park Y. Robust H ∞ preview control of an active suspension system with norm-bounded uncertainties. Int J Automot Technol. 2008;9:585–592. DOI:10.1007/s12239-008-0069-7.

[11] Tseng HE, Hrovat D. State of the art survey: active and semi-active suspension control. Vehicle System Dynamics. 2015;53:1034–1062. DOI:10.1080/00423114.2015.1037313.

[12] Streiter R. Active preview suspension system. ATZ Worldw. 2008;110:4–11. DOI:10.1007/BF03225003.

[13] Schindler A. New conception and first-time implementation of an active chassis with a preview strategy [Internet]. KIT Scientific Publishing; 2009 [cited 2024 Jan 15]. Available from: https://publikationen.bibliothek.kit.edu/1000013552.

[14] Bouzouraa ME, Kellner M, Hofmann U, et al. Laser scanner based road surface estimation for automotive applications. Sensors 2014 IEEE. December 2014; Valencia, Spain. 2034–2037. DOI:10.1109/ICSENS.2014.6985434.

[15] Gong M, Wang H, Wang X. Active Suspension Control Based on Estimated Road Class for Off-Road Vehicle. Math Probl Eng. 2019;2019. DOI:10.1155/2019/3483710.

[16] Stein GP, Stein GP, Mano O, et al. A Robust Method for Computing Vehicle Ego-motion. IEEE Intell Veh Symp, Dearborn, MI, USA, 2000;362-368. DOI:10.1109/IVS.2000.898370.

[17] Göhrle C, Schindler A, Wagner A, et al. Road Profile Estimation and Preview Control for Low-Bandwidth Active Suspension Systems. IEEE/ASME Trans Mechatronics. 2015;20:2299–2310. DOI:10.1109/TMECH.2014.2375336.

[18] Weist U, Missel J, Cytrynski S, et al. Fahrkomfort der extraklasse. ATZextra. 2013;18:124–128. DOI: 10.1365/s35778-013-0060-4.

[19] Shen T, Schamp G, Haddad M. Stereo vision based road surface preview. 17th IEEE Int Conf Intell Transp Syst ITSC 2014. Qingdao, China, 2014;1843–1849. DOI:10.1109/ITSC.2014.6957961.

[20] Pfeiffer D, Gehrig S, Schneider N. Exploiting the Power of Stereo Confidences. 2013 IEEE Conference on Computer Vision and Pattern Recognition, Portland, OR, USA, 2013;297-304. DOI:10.1109/CVPR.2013.45.

[21] Hu X, Mordohai P. A quantitative evaluation of confidence measures for stereo vision. IEEE Trans Pattern Anal

Mach Intell. 2012;34:2121–2133. DOI:10.1109/TPAMI.2012.46.

[22] Suhr JK, Jung HG. Dense stereo-based robust vertical road profile estimation using hough transform and dynamic programming. IEEE Trans Intell Transp Syst. 2015;16:1528–1536. DOI:10.1109/TITS.2014.2369002.

[23] Lee JK, Yoon KJ. Temporally Consistent Road Surface Profile Estimation Using Stereo Vision. IEEE Trans Intell Transp Syst. 2018;19:1618–1628. DOI:10.1109/TITS.2018.2794342.

[24] Deigmoeller J, Einecke N, Fuchs O, et al. Road surface scanning using stereo cameras for motorcycles. VISIGRAPP 2018 - Proc 13th Int Jt Conf Comput Vision, Imaging Comput Graph Theory Appl. 2018;5:549–554. DOI:10.5220/0006614805490554

[25] Schindler A, Göhrle C, Sawodny O. Method for precise scaling of an image of a camera sensor and system. European Patent EP2916102B1. 2019 Oct 23 [cited 2024 Jan 15]. Available from: https://data.epo.org/gpi/EP2916102B1-METHOD-FOR-PRECISE-SCALING-OF-AN-IMAGE-OF-A-CAMERA-SENSOR-AND-SYSTEM.

[26] Sander J. Density-Based Clustering. Encyclopedia of Machine Learning. 2011;270–273. DOI:10.1007/978-0-387-30164-8_211.

[27] Braune C, Besecke S, Kruse R. Density based clustering: Alternatives to DBSCAN. Partitional Clust Algorithms. Springer International Publishing. 2015;193–213. DOI:10.1007/978-3-319-09259-1_6.

[28] Savaresi S, Poussot-Vassal C, Spelta C, et al. Semi-Active Suspension Control Design for Vehicles. 1st ed. Butterworth-Heinemann. 2010;71–90.

[29] Shimoya N, Katsuyama E. A Study of Triple Skyhook Control for Semi-Active Suspension System. SAE Technical Paper 2019-01-0168. 2019. DOI:10.4271/2019-01-0168.

[30] Büyükköprü M, Uzunsoy E, Mouton X. Yol Profili Kestirimi Yapılmasını Sağlayan Metot [Method That Enables Road Profile Estimation]. Türk Patent 2021 009190. 2023 Oct 23 [cited 2024 Jan 15]. Available from: https://portal.turkpatent.gov.tr/anonim/arastirma/patent/sonuc/dosya?patentAppNo=2021/009190&documentsTpye=all.

[31] Ester M, Kriegel H-P, Sander J, et al. A Density-Based Algorithm for Discovering Clusters in Large Spatial Databases with Noise. KDD'96: Proceedings of the Second International Conference on Knowledge Discovery and Data Mining. 1996;226-231.

[32] Schubert E, Sander J, Ester M, et al. DBSCAN Revisited, Revisited: Why and How You Should (Still) Use DBSCAN. ACM Transactions on Database Systems. 2017;42:1-21. DOI:10.1145/3068335.